Nonlin. Processes Geophys., 13, 185–203, 2006
www.nonlin-processes-geophys.net/13/185/2006/

Nonlinear Processes in Geophysics

Influence of stability on the flux-profile relationships for wind speed, ϕ_m, and temperature, ϕ_h, for the stable atmospheric boundary layer

C. Yagüe[1], **S. Viana**[1], **G. Maqueda**[2], **and J. M. Redondo**[3]

[1]Dpto. Geofísica y Meteorología, Universidad Complutense de Madrid, Spain
[2]Dpto. Astrofísica y Ciencias de la Atmósfera, Universidad Complutense de Madrid, Spain
[3]Dpto. Física Aplicada, Universidad Politécnica de Catalunya, Barcelona, Spain

Received: 1 August 2005 – Revised: 21 April 2006 – Accepted: 21 April 2006 – Published: 21 June 2006

Part of Special Issue "Turbulent transport in geosciences"

Abstract. Data from SABLES98 experimental campaign have been used in order to study the influence of stability (from weak to strong stratification) on the flux-profile relationships for momentum, ϕ_m, and heat, ϕ_h. Measurements from 14 thermocouples and 3 sonic anemometers at three levels (5.8, 13.5 and 32 m) for the period from 10 to 28 September 1998 were analysed using the framework of the local-scaling approach (Nieuwstadt, 1984a; 1984b), which can be interpreted as an extension of the Monin-Obukhov similarity theory (Obukhov, 1946). The results show increasing values of ϕ_m and ϕ_h with increasing stability parameter ζ=z/Λ, up to a value of $\zeta \approx$1–2, above which the values remain constant. As a consequence of this levelling off in ϕ_m and ϕ_h for strong stability, the turbulent mixing is underestimated when linear similarity functions (Businger et al., 1971) are used to calculate surface fluxes of momentum and heat. On the other hand when ϕ_m and ϕ_h are related to the gradient Richardson number, R_i, a different behaviour is found, which could indicate that the transfer of momentum is greater than that of heat for high R_i. The range of validity of these linear functions is discussed in terms of the physical aspects of turbulent intermittent mixing.

1 Introduction

Turbulent transfer is one of the most important processes in geophysical flows, which is characterized by a high degree of nonlinearity (Redondo et al., 1996). For the atmosphere, this turbulent transport takes place mainly in its lower part, near to the ground where important interactions occur: the Atmospheric or Planetary Boundary Layer (ABL or PBL). This ABL shows stratification which is often stable during the night in mid-latitude sites (Yagüe and Cano, 1994a) and can exist for prolonged periods during the months of winter darkness at polar places (King and Anderson, 1988; 1994; Yagüe and Redondo 1995). In these conditions surface inversions are common and sometimes very strong, suppressing vertical turbulent mixing which can be very dangerous in polluted atmospheres (Morgan and Bornstein, 1977; Jacobson, 2002). Stable stratification can also lead to pollution problems in the ocean (Rodriguez et al., 1995). Surface based inversions are developed not only over the ground but also over the ocean, due to warm air advection over colder water, producing a stable atmospheric boundary layer over the ocean (Lange et al., 2004).

The quantities most frequently used within the ABL, for atmospheric dispersion and forecasting models, are surface fluxes of momentum and heat. These surface fluxes are very important because of their strong influence on the mean profiles in the lower atmosphere. Moreover, exchange coefficients and boundary layer heights, which are needed as input for air pollution models, depend on the surface fluxes (Beljaars and Holtslag, 1991). In order to describe these fluxes (momentum and heat are the most common but the procedure can be extended to any particular property such as pollutants, humidity, etc), formulas for non-dimensional wind and temperature gradients (the so-called universal similarity functions) are used. These formulas result from the application of the Monin-Obukhov (M-O) similarity theory (1954) which is a suitable framework for presenting micrometeorological data, as well as for extrapolating and predicting certain micrometeorological information when direct measurements of turbulent fluxes are not available (Arya, 2001). The similarity functions for momentum, ϕ_m, and heat, ϕ_h, are a fundamental tool to obtain estimations of the surface fluxes. These surface fluxes are often used to parameterize the mixing height in some meteorological simulations, and this is one of the most critical parameters in the evaluation of the pollution models, as the mixing rate of atmospheric pollutants is controlled by the variation of this

Correspondence to: C. Yagüe
(carlos@fis.ucm.es)

Published by Copernicus GmbH on behalf of the European Geosciences Union and the American Geophysical Union.

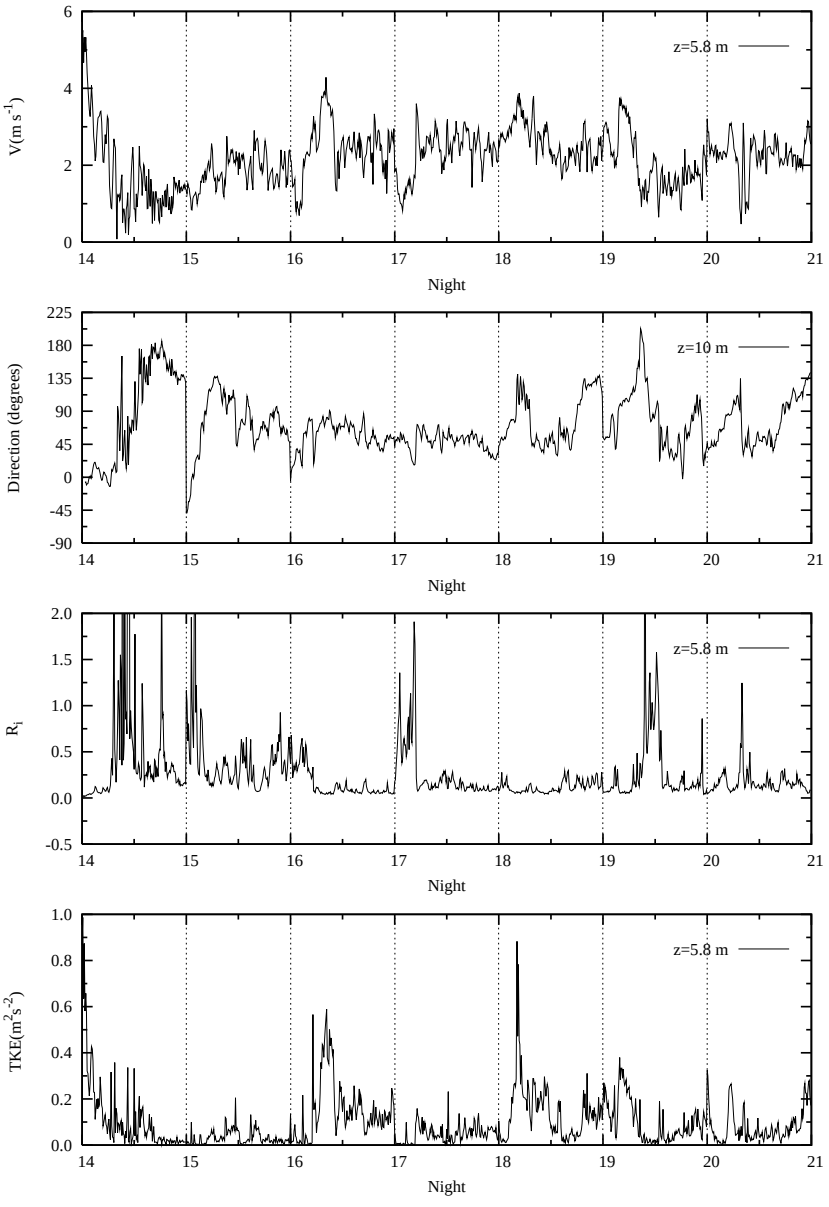

Fig. 1. Evolution of wind speed (5.8 m) and direction (10 m), Richardson number (5.8 m) and TKE (5.8 m) for the nights of the S-Period only.

mixing height (Berman et al., 1997). For unstable and neutral conditions good agreements between direct measurements and those evaluated from the similarity functions have been found (Businger et al., 1971; Hicks, 1976; Högström, 1988; Sugita and Brutsaert, 1992). However under stable conditions the results are not so good, especially for weak winds where strong stratification takes place (Lee, 1997; Sharan et al., 2003). This difference between unstable and stable conditions is produced because turbulent fluxes are much larger for convective conditions than for stable ones (Cheng and Brutsaert, 2005).

Several processes in the Stable Boundary Layer (SBL) make this case much more difficult to study and to understand (Finnigan et al., 1984; Mahrt, 1989; Yagüe and Cano, 1994b; Mahrt et al., 1998; Cuxart et al., 2000, Poulos et al., 2002): weak and intermittent turbulence, the presence of internal waves, non-linear interactions between turbulence and waves, Kelvin-Helmholtz instabilities, development of low-level jets, production of elevated turbulence, katabatic flows, etc. Intermittency is not a clearly defined concept and it is quite sensitive to detection criteria (Klipp and Mahrt, 2004). Some authors attribute the intermittency to external forcing such as internal gravity waves, density

Table 1. Some of the instrumentation used at SABLES98 100 m tower.

Instrument	z(m)	Sample freq.(Hz)	Threshold	Accuracy
Sonic anemometers	5.8-13.5-32	20	15 mm/s for u,v 4mm/s for w	±3%
Wind vanes	10-20-100	5	1 m/s	±3%
Cup anemometers	3-10-20-50-100	5	0.5 m/s	±0.2 m/s
Thermistor	10	1		±0.1°C
Platinum resistance thermometers	10–20, 20–50	1		±0.1°C
Thermocouples	0.22-0.88-2-3.55-5.55-8-10.88-14.22-18-22.22-26.88-32-37.55-43.55-50	5		±0.03°C

currents, low level jets or perhaps mesoscale processes, while others associate intermittency with interactions between turbulence and local mean gradients (Derbyshire, 1999). On the other hand, some authors (Zilitinkevich and Calanca, 2000; Zilitinkevich, 2002; Sodemann and Foken, 2004) have extended the theory of the atmospheric SBL by a distinction between nocturnal and long-lived stable boundary layers (winter polar regions). In the latter, the free atmosphere may influence the fluxes in the surface layer, and this would require a modification of the traditional M-O similarity theory which is taken into account by introducing the Brunt-Väisalä frequency in the similarity functions. Esau (2004) evaluated the non-local effect of the ambient atmospheric stratification on the parameterization of the surface drag coefficient, as the classical parameterization fails to estimate the turbulent exchange. We will estimate intermittency from velocity probability distribution functions and structure function analysis as described in Mahjoub et al. (1998).

With all these considerations in mind, we have evaluated here the flux-profile relationships for a wide range of stability from SABLES98 data, analyzing the consequences of using some of the common functions to evaluate turbulent fluxes out of their range of validity. In the next section a brief description of the site where the experimental campaign took place and the instrumentation used will be given. In section 3 we present the methodology used to calculate the behaviour of ϕ_m and ϕ_h versus the local stability parameter z/Λ. In Sect. 4 the main results of the study are presented and in Sect. 5 we discuss the mixing processes and intermittency related to the stability conditions and the turbulent Prandtl number. Finally the conclusions are presented relating our results to previous work in the ABL and laboratory and numerical experiments.

2 Site and measurements

The data used in this study is part of the SABLES98 (Stable Atmospheric Boundary Layer Experiment in Spain) field campaign which took place in September 1998 (from 10 to 28) at the Research Centre for the Lower Atmosphere (CIBA), situated at 840 m above sea level on the Northern Spanish Plateau. The surrounding terrain is fairly flat and homogeneous. The Duero River flows along the SE border of the plateau; two small river valleys, which may act as drainage channels in stable conditions, extend from the lower SW region. The place is surrounded by mountain ranges approximately 100 km distant extending from the SE to the North. Katabatic flows may be generated in the air flow over the mountainous terrain (Cuxart et al., 2000). In the present study we have concentrated on the so-called S-period (Stable period) comprising seven consecutive nights (from 18:00 GMT to 06:00 GMT) ranging from the night from 14 to 15 September to that from 20 to 21 September. The synoptic conditions were controlled by a High pressure system which produced light winds mainly from the NE-E direction.

Different instruments (3 sonic and 5 cup anemometers, 14 thermocouples, 3 wind vanes, etc) were deployed on a 100 m high tower. A summary of technical specifications and the heights at which these instruments were installed are given in Table 1. For further information on SABLES98 Cuxart et al. (2000) should be consulted. Five-minute means have been used to evaluate all the parameters in this study, which were provided (and calibrated) by the Risoe National Laboratory.

In order to appreciate the main characteristics of the S-period, the evolution of wind speed and direction, the gradient Richardson number and turbulent kinetic energy near the ground are shown in Fig. 1. Notice that only nocturnal periods (from 18:00 GMT to 06:00 GMT) are drawn. In spite of a similar synoptic situation throughout the entire S-period, the stability (evaluated from the gradient Richardson number) and turbulence varied substantially because both, stability and turbulence, are very sensible to wind speed near the ground and small changes in wind can produce different

levels of turbulence. Periods with higher stability, which corresponds to higher values of the Richardson number, low turbulent kinetic energy (TKE), and low surface winds, can be found for the nights of 14–15, 15–16, beginning of 17–18 and 20–21 September. The average wind direction is East, ranging from N to SE, and might be attributed mainly to local and orographic effects, most likely to drainage flows. However, when different evolutions are analysed in detail, the interaction of turbulence and waves can be present and some stable records are sometimes interrupted by peaks of TKE. Such peaks could be produced by the breaking of internal gravity waves, which can generate strong local turbulence and increase the intermittency. These arguments are further explained below, see also Redondo et al. (1996), Yagüe et al. (2004).

3 Methodology

This study has been developed in the framework of the local-scaling approach, which can be interpreted as an extension of the M-O similarity to the stable boundary layer (Nieuwstadt, 1984a, 1984b; Forrer and Rotach, 1997; Howell and Sun, 1999) when turbulent and stability local values are used instead of surface values.

Turbulent fluxes of momentum (τ) and heat (H) can be calculated directly from eddy correlation measurements or from velocity (u_*) and temperature scales (θ_*):

$$\tau = -\rho\overline{u'w'} = \rho u_*^2 \tag{1}$$

$$H = \rho c_p \overline{w'\theta'} = -\rho c_p u_* \theta_* \tag{2}$$

where ρ is the density and c_p the specific heat for constant pressure. The covariances $\overline{u'w'}$ and $\overline{\theta'w'}$ are directly evaluated from the sonic anemometer measurements.

The similarity functions (ϕ_m and ϕ_h) for momentum and heat are defined as non-dimensional forms of the mean wind speed and potential temperature gradients:

$$\phi_m(\zeta) = \frac{kz}{u_*}\frac{\partial \overline{u}}{\partial z} \tag{3}$$

$$\phi_h(\zeta) = \frac{kz}{\theta_*}\frac{\partial \overline{\theta}}{\partial z} \tag{4}$$

where $\overline{u}$ and $\overline{\theta}$ are mean wind speed and potential temperature, respectively, k the von Karman constant, z height, u_* friction velocity (related to turbulent momentum flux) and θ_* the scale temperature (related to turbulent heat flux) as mentioned above. $\zeta = z/L$ is a stability parameter defined as the ratio of height, z, to a length scale L known as Monin-Obukhov length:

$$L = \frac{-u_*^3}{k(g/T_0)(H_0/\rho c_p)} \tag{5}$$

with T_0 a reference temperature (near the surface), H_0 the surface heat flux and g the acceleration due to gravity. L is a measure of the height of the dynamical influence layer where surface properties are transmitted ($z<L$). For $z>L$ the thermal influence is the dominant factor.

By using local-scaling, dimensional combinations of variables measured at the same height can be expressed as a function of a single independent parameter, z/Λ. The scale Λ is evaluated from Eq. (5) but replacing the surface u_* by the local friction velocity, and H_0 by the local heat flux. Λ is generally dependent on height, while L is constant in the surface layer, so that $\Lambda(0)$=L. Similarly, ϕ_{m} and ϕ_{h} can be evaluated from local values of u_*, θ_* and local gradients of wind speed and potential temperature. This has been the procedure in this study. All the parameters have been calculated using the local values at each corresponding height (the 3 levels of the sonic anemometers, 5.8 m, 13.5 m and 32 m.). For the purpose of simplicity z/Λ has been denoted as ζ. The M-O relationships become local-scaling if the heat flux and stress at level z are significantly different from the surface values. When the instruments at level z are in the surface layer, the M-O surface-layer scaling and local scaling are approximately the same; if not, the fluxes at that level are lower than at the surface and M-O similarity does not apply (Klipp and Mahrt, 2004). In our study, where moderate to high stability often appears, the surface layer can be below the 3 levels used. Normally the covariance $\overline{v'w'}$ is quite small when the reference system of coordinates takes u as the wind in the mean direction, and v perpendicular to it, but for completeness it is used when available, and then the friction velocity, u_*, is evaluated as:

$$u_* = \left[(-\overline{u'w'})^2 + (-\overline{v'w'})^2\right]^{1/4} \tag{6}$$

The temperature scale, θ_*, can be directly evaluated from:

$$\theta_* = \left[\frac{\overline{w'\theta'}}{-u_*}\right] \tag{7}$$

When the covariances ($\overline{u'w'}$, $\overline{v'w'}$ and $\overline{\theta'w'}$) are not available, then turbulent fluxes of momentum and heat can be estimated from u_* and θ_*, which are evaluated from standard vertical profiles of mean values of wind speed and potential temperature using Eq. (3) and (4) once the functions $\phi_{\mathrm{m}}(\zeta)$ and $\phi_{\mathrm{h}}(\zeta)$ are known. In this case, ζ is also estimated from standard mean values of temperature and wind through the gradient Richardson number:

$$Ri = \frac{\frac{g}{\theta_0}\frac{\partial \overline{\theta}}{\partial z}}{\left(\frac{\partial \overline{u}}{\partial z}\right)^2} \tag{8}$$

Using forms (3), (4) and (8), a relationship between ζ and R_i is directly found as:

$$Ri = \frac{\zeta \phi_h(\zeta)}{\phi_m^2(\zeta)} \tag{9}$$

Table 2. Original functions ϕ_m=1+$\beta_1\zeta$ and ϕ_h=α+$\beta_2\zeta$ for different authors in stable conditions, and their modified forms (Högström, 1996) considering a value of k=0.4 (von Karman constant)

Reference	k	β_1	α	β_2
Businger et al. (1971)				
Original	0.35	4.7	0.74	4.7
Modified (Högström, 1996)	0.40	6	0.95	7.99
Dyer (1974)				
Original	0.41	5.0	1	5
Modified (Högström, 1996)	0.40	4.8	0.95	4.5
Zilitinkevich and Chailikov (1968)				
Original	0.43	9.9	1	9.9
Modified (Högström, 1996)	0.40	9.4	0.95	8.93
Webb (1970)				
Original	0.41	5.2	1	5.2
Modified (Högström, 1996)	0.40	4.2	0.95	7.03
Hicks (1976)				
Original	0.41	5.0	1	5

which will be discussed in Sects. 4 and 5.

For each 5-min block of data, $\overline{u}$(z) and $\overline{\theta}$(z) profiles were obtained from fitting a log-linear curve to the data:

$$\overline{u}=az+b\ln z+c$$
$$\overline{\theta}=a'z+b'\ln z+c' \quad (10)$$

The correlation coefficient of these fits was generally very high (>0.98), and only for some near-neutral conditions with strong winds the goodness of the fit for potential temperature decreased; in this case, fits with a correlation coefficient less than 0.9 have been excluded. Nieuwstadt (1984b) showed that the log-linear profile is the accepted profile in the stable surface layer and King (1990), Yagüe and Cano (1994a), Forrer and Rotach (1997), and Cuxart et al. (2000) used them subsequently. If ϕ_m and ϕ_h are integrated over z, a log-linear profile of u and θ is obtained.

From these fits, the gradient of wind speed and potential temperature are directly obtained for each level of interest as:

$$\frac{\partial\overline{u}}{\partial z}=a+\frac{b}{z}$$
$$\frac{\partial\overline{\theta}}{\partial z}=a'+\frac{b'}{z} \quad (11)$$

The levels used to obtain the fits were: 3.0, 5.8, 10.0, 13.5, 20, 32 and 50 m (for wind speed), and 0.88, 3.55, 5.55, 8, 10.88, 14.22, 18, 22.22, 26.88, 32, 37.55, y 43.55 m (for temperature).

Then vertical gradients were evaluated for the heights of interest, 5.8 m, 13.5 m and 32 m. With these gradients and u_* and θ_* evaluated from Eqs. (6) and (7), ϕ_m and ϕ_h were directly obtained for the three heights using Eqs. (3) and (4). Functional forms for ϕ_m and ϕ_h were then obtained for a wide range of stabilities ($0<\zeta<50$) and compared with those widely used in the literature (Table 2 shows some of these universal functions). Högström (1988; 1996) revised some of these linear relations of $\phi_m(\zeta)$ and $\phi_h(\zeta)$ for different values of von Karman constant (k), establishing the slopes of the different relationships for k=0.40, which is widely accepted. Beljaars and Holtslag (1991) proposed a nonlinear formulation of $\phi_m(\zeta)$ and $\phi_h(\zeta)$ which has recently been used in some numerical studies (Basu, 2004). Handorf et al. (1999) confirmed the linear relations of the universal functions in the framework of the surface-layer and local-scaling for $\zeta<0.8$–1 using the FINTUREX94 data. They mention that measurements in the range of $\zeta>2$ cannot be found in the literature, since the SBL is not often that stable and the results are statistically uncertain; this underlines the importance of this kind of studies, it is precisely in strongly stratified situations when vertical mixing is inhibited and intermittency is strongest.

4 Results

In this section we summarize the results obtained grouped in four subsections. First of all the influence of local stability (ζ=z/Λ) on the non-dimensional gradient of wind speed, ϕ_m, will be analyzed. Subsequently the behaviour of the non-dimensional gradient of potential temperature, ϕ_h, will be studied, following with the relationship between the two stability parameters, the gradient Richardson number and ζ, which are frequently used in the micrometeorological literature (Launiainen, 1995). Finally the relationships between ϕ_m, ϕ_h and the gradient Richardson number will be shown.

In many of the figures, log-log plots have been used to present the results because several parameters exhibit a range of values extending several orders of magnitude. Moreover and in order to improve convergence of statistics, some of the results have been grouped into z/Λ intervals. Unless stated

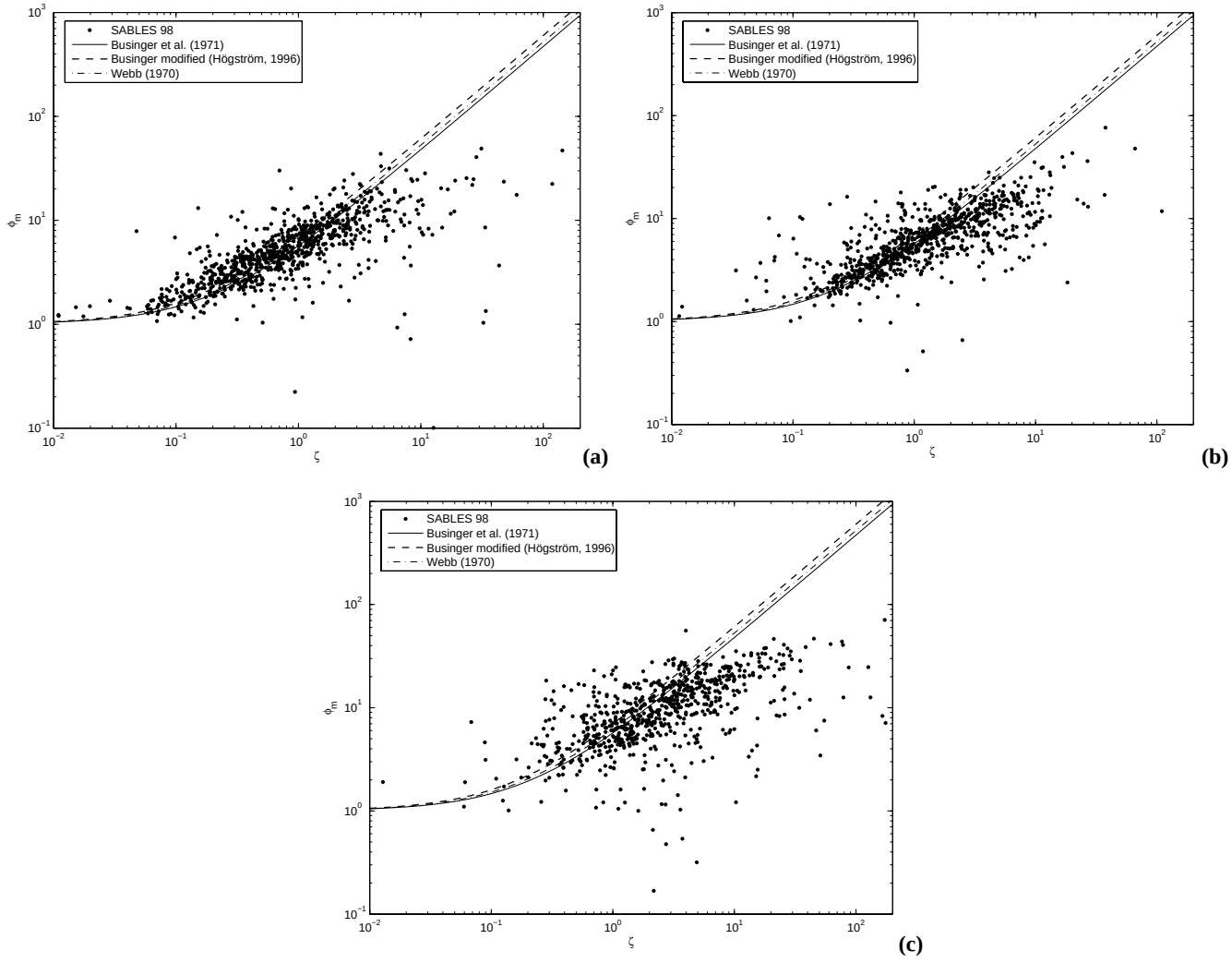

Fig. 2. ϕ_m versus stability parameter for all the values calculated (S-period) at : **(a)** 5.8 m, **(b)** 13.5 m and **(c)** 32 m. Functions found by other authors are shown for comparison.

otherwise, these intervals are: (<0.05), (0.05–0.1), (0.1–0.2), (0.2–0.3), (0.3–0.4), (0.4–0.5), (0.5–0.7), (0.7–1), (1–1.5), (1.5–2), (2–3), (3–4.5), (4.5–7), (7–10), (10–15), (15–20), (20–30), (>30). The criterion of Mahrt (1999) was adopted to establish different degrees of stability: weak stability for $\zeta \leq 0.1$, moderate stability for $0.1 < \zeta \leq 1$ and strong stability for $\zeta > 1$. The value of ζ to distinguish between weak and moderate stability is obtained locating the maximum of the downward heat flux in stable conditions. While Mahrt obtained 0.06 at z=10 m, Grachev et al. (2005) showed that it depends on z, obtaining $z/\Lambda \approx 0.02$ for z=2 m., and $z/\Lambda \approx 0.1$ for z=5 and 14 m. Considering the range of possible values, we chose an approximation of ζ=0.1 as our criterion.

4.1 Flux-profile relationship for wind speed (ϕ_m)

The relationship between ϕ_m and ζ for all the data analyzed for the S-period of SABLES98 can be seen in Fig. 2 for the three heights studied (5.8 m, 13.5 m and 32 m). Businger et al. (1971) – original and modified by Högström (1988)- and Webb (1970) have been drawn for comparison because these are probably the most widely used in the literature. If all the linear functions showed in Table 2 would have been drawn, no important differences would have been found. The data are more scattered as the height is increased, especially at 32 m in Fig. 2c where the points are less grouped around Businger's and Webb's lines.

As stability (ζ) increases, intermittent turbulence is more frequent, fluxes are decoupled from the surface values (Yagüe and Redondo, 1995), and the phenomenon of z-less stratification (Nieuwstadt, 1984a; 1984b) is present: ζ is not controlling the momentum flux and ϕ_m tends to level off. Nieuwstadt explains this levelling off as the limit of validity of the local-scaling for $z/\Lambda \rightarrow \infty$. Stable stratification inhibits vertical motions and as a result reduces the length scale

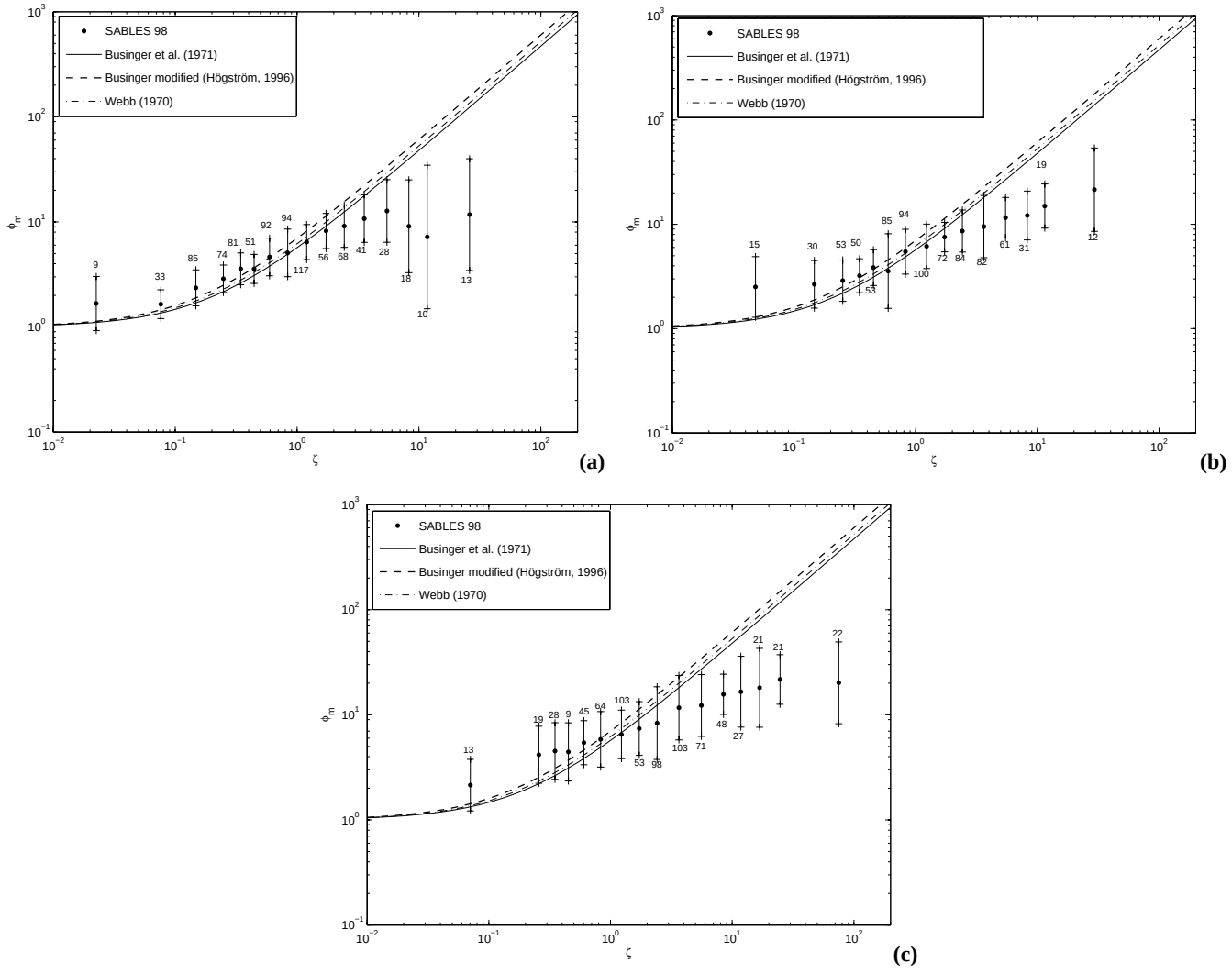

Fig. 3. ϕ_m versus stability parameter grouped into intervals for the S-Period, at: **(a)** 5.8 m, **(b)** 13.5 m and **(c)** 32 m. Functions found by other authors are shown for comparison. Error bars indicate the standard deviation of the individual results contributing to the mean value in each stability bin. The number of samples in each stability bin is given over the upper bar or below it.

of turbulence. When this length scale becomes much smaller than the height above surface, z, turbulence no longer feels the presence of the ground and as a consequence an explicit dependence on z disappears. The length scale of turbulence is proportional to Λ and in terms of local scaling this result means that dimensionless quantities approach a constant value for large z/Λ. Then when stability is high (for large values of z/Λ) it is logical to think that there is a decoupling from the surface at relatively short heights (and these heights are probably over the surface layer).

The scaling and the onset of z-less stratification are better seen if the data are grouped in intervals listed in section 4 above (Fig. 3). Where intervals contained too few samples, the data groups were combined: the first interval for z=13.5 m is $\zeta<0.1$, and for z=32 m is $\zeta<0.2$; on the other hand the last interval for z=5.8 m and 13.5 m is $\zeta>15$, and for z=32 m $\zeta>30$. The best agreement between SABLES98 data and Businger's functions is found for z=5.8 m, for weak to moderate stability. It is in this zone where error bars are shorter and Businger's and Webb's functions are within these bars. A possible reason for this behaviour is that z=5.8 m is the closest level to the ground and it is more probable to be inside the surface layer, which is the portion of the ABL where the M-O theory (leading to the flux-profile relationships) is fulfilled. Högström (1988) found an indication of the levelling off for ϕ_m in the range $0.5<\zeta<1$, but with few data points and a large scatter. Howell and Sun (1999) found that ϕ_m levelled off for ζ around 0.5 for measurements at z=10 m, irrespective of whether a cut-off time scale of 10 min or a variable cut off time scale was used to calculate the fluxes. Handford et al. (1999) found for Antarctic data that, at z=4.2 m, ϕ_m is $\cong$ constant for $\zeta>0.8$, but with

Table 3. Linear fits for ϕ_m against ζ (mean values) for $\zeta<2$. a and β_1 are the coefficients of the fit, Δa and $\Delta\beta_1$ are the errors in the estimation of these coefficients, and R is the correlation coefficient.

Level	a	Δa	β_1	$\Delta\beta_1$	R
5.8 m	2.05	0.17	4.05	0.22	0.9883
13.5 m	2.69	0.2	3.17	0.25	0.9779
32 m	3.9	0.5	3.0	0.5	0.9078

Table 4. Linear fits of ϕ_m at z=5.8 m from the whole data for $\zeta<2$.

Level	a	Δa	β_1	$\Delta\beta_1$	R
5.8 m	2.17	0.14	3.96	0.17	0.6537

a large scatter, whereas at z=1.7 m that tendency could not be indicated due to the missing measurements. Cheng and Brutsaert (2005) found for CASES99 data that the stability functions show a linear behaviour up to a value of ζ=0.8, but for stronger stabilities both functions (ϕ_m and ϕ_h) approach a constant with a value of approximately 7.

Another point to underline is that, for the three levels analysed, the mean values of SABLES98 slightly overestimate the values given by Businger functions for ζ approximately less than 1, and underestimate for ζ greater than 1. The value of ζ=1 corresponds to z=Λ, i.e. when the local M-O length (height of the dynamical influence layer) is equal to the height where ϕ_m is evaluated (5.8 m, 13.5 m and 32 m). The points to the left of ζ=1 ($\Lambda>z$) are within the layer of dynamical influence from the ground in each case but for the points to the right, $z>\Lambda$, decoupling from the surface is more likely, the intermittency increases, and a higher tendency to z-less stratification is found (Nieuwstadt, 1984a, 1984b). This is important to take into account when the flux-profiles relationships are used to calculate surface fluxes of momentum and heat in the stable atmospheric boundary layer. Most of times linear similarity functions are used (see Table 2), but for strong stability (light nocturnal winds) this can produce large errors in the estimation of the fluxes. Different meteorological models used for dispersion studies or forecasting meteorological parameters make use of Businger et al. (1971) functions or other similar (Webb, 1970; Dyer, 1974) to obtain surface layer parameters as u_*, θ_* and L:

$$u_*=\frac{kz}{\phi_m}\frac{\partial\overline{u}}{\partial z} \tag{12}$$

$$\theta_*=\frac{kz}{\phi_h}\frac{\partial\overline{\theta}}{\partial z} \tag{13}$$

If ϕ_m and ϕ_h are overestimated (and this happens for strong stability as it is shown in Fig. 3) then u_* and θ_* are underestimated and also the fluxes calculated from them. This was pointed out by Louis (1979) using a weather forecasting model where Dyer's similarity functions were used. As a consequence of having underestimated the surface fluxes of momentum and heat, the surface cooling could be several degrees below the observed values. Some climatic models (Noguer et al.,1998) have shown this problem for seasons and places where the atmospheric boundary layer is strongly stable.

A comparison of Fig. 3a (5.8 m) with Fig. 3c (32 m) shows that the lower level contains many more points with $\zeta<0.1$ than the upper level while the opposite is found for $\zeta>1$ which would support the general idea of increasing stability with height.

A further point to note from Fig. 3 is that the mean values of ϕ_m seem to be significantly greater than Businger and Webb functions for the lowest intervals of ζ. However, this must be viewed in the context that this interval contains very few points (e.g. 9 points at 5.8 m). If a wider nocturnal period is considered, namely the entire period from 10 to 26 September (see Fig. 4) where near-neutral stability is also included, the mean values for small ζ agree well with Businger′s and Webb′s functions, especially at the two lower heights (z=5.8 m in Fig. 4a and z=13.5 m in Fig. 4b). As it will be shown in the next subsection, this effect (even greater) is also apparent for ϕ_h. A possible explanation is related to the few data found in the S-period for these low values of ζ, which are not enough to obtain a significant statistic, and also to the influence of the global stability on the mixing processes; these few points are probably "contaminated" by a bulk stability and they are not truly near-neutral (as it was the case of the Businger and Webb datasets).

The general behaviour of ϕ_m increasing with stability until a certain value of ζ approx. 1–2, followed by a levelling off is in agreement with other relationships found in the literature for other locations (Forrer and Rotach, 1997; Howell and Sun, 1999; Yagüe et al., 2001; Klipp and Mahrt, 2004; Cheng and Brutsaert, 2005), and would support the z-less theory, initially proposed by Wyngaard (1973) and extended by Nieuwstadt (1984a, 1984b).

Finally, a specific similarity function of the form ϕ_m=a+$\beta_1\zeta$ was fitted to the mean values of SABLES98 data (S-period, shown in Fig. 3) for $\zeta<2$ for the three levels studied (see Fig. 5). A summary of the three fits evaluated can be seen in Table 3. It can be observed that different fits are found for the three levels, showing once more the importance of using local-scaling when stability is even weak to moderate in the global context of a stable situation like it is the S-period. The linear fit with smallest errors and largest correlation coefficient is that obtained for the lowest level (5.8 m), and it is also the fit closer to Businger et al. (1971). The high values found for the correlation coefficient are due to the fact of having done the fit to the mean values. If the fit is done to the whole data points (for $\zeta<2$ and at z=5.8 m, see Fig. 6) the results can be found in Table 4; coefficients a and β_1 are

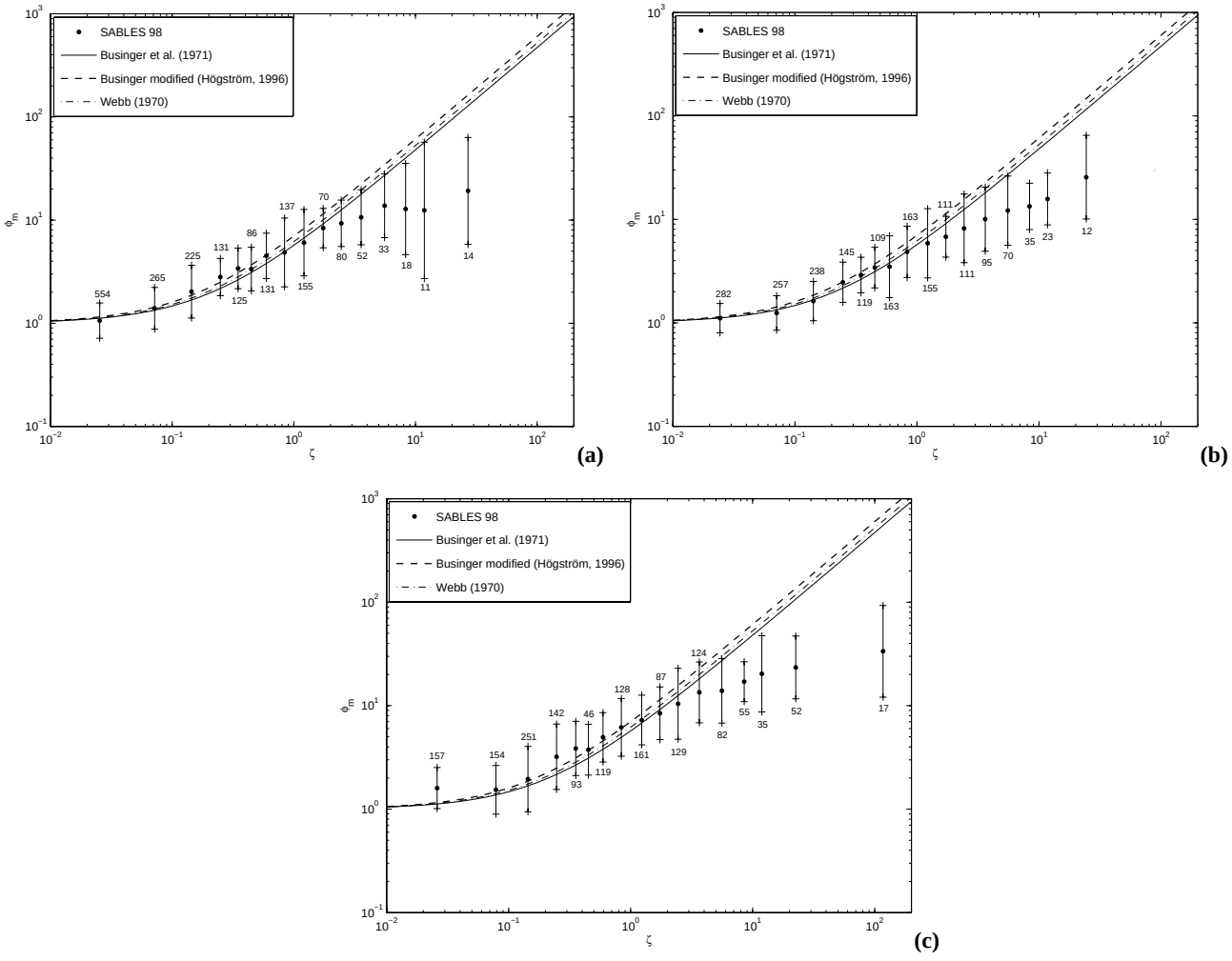

Fig. 4. As Fig. 3, but for the extended nocturnal period from 10 to 26 September.

similar to those obtained previously for the mean data, but the correlation coefficient is considerably lower.

It is also interesting to comment that Klipp and Mahrt (2004) found for CASES99 data that the correlation between ϕ_m and ζ for stable conditions is strongly influenced by self-correlation. This self-correlation is evident for all values of ζ but is more significant for the largest values of stability, where the scatter of the data is large. They established that the reduction of ϕ_m below the linear prediction in strongly stable data could be due to self-correlation. Klipp and Mahrt (2004) proposed that if the gradient Richardson number is used as a stability parameter, these figures would suffer less from self-correlation; although there is also a self-correlation (vertical gradient of wind speed is the shared variable), it is much less compared to using ζ, due to the fact that the range of shear data is relatively small compared to turbulent fluxes, whereas it is the friction velocity which is the shared variable when ζ is used as stability parameter. An analysis of the similarity functions versus gradient Richardson number will be shown below in Sect. 4.4.

4.2 Flux-profile relationship for temperature (ϕ_h)

In this section, the dependence of the dimensionless gradient of potential temperature, ϕ_h, on the stability parameter is discussed. As Fig. 7 shows, the results are much more scattered than those obtained for ϕ_m which could be attributed to several reasons: Duynkerke (1999) related this effect to the lower accuracy in the determination of the temperature gradients compared to those of wind speed. Another reason could be that the local gradient of potential temperature can be close to zero at lower stability, introducing larger errors in the evaluation of ϕ_h. Handorf et al. (1999) showed large values of ϕ_h at z=4.2 m for ζ <0.01, compared to those predicted by the linear functions, but no explanation was given. Yagüe et al. (2001) also found greater scatter for ϕ_h than for ϕ_m using Antarctic data, and large values of ϕ_h for near-neutral conditions. It was clear that the increase in scatter for

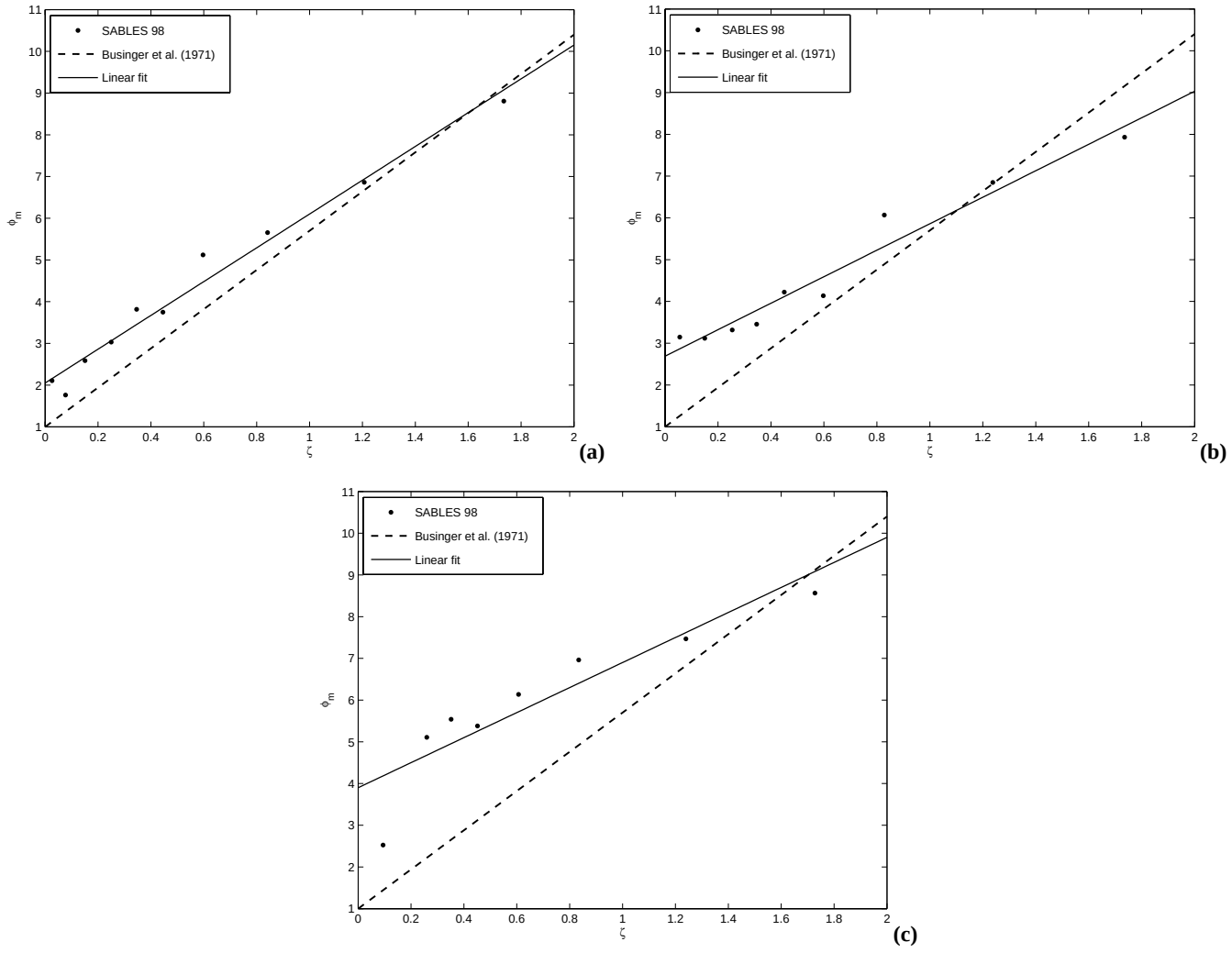

Fig. 5. Linear fits of ϕ_m mean values versus ζ for stability parameter <2 at: **(a)** 5.8 m, **(b)** 13.5 m and **(c)** 32 m. Businger et al. (1971) function is shown for comparison.

higher Richardson numbers was not due to undersampling. The scatter in both, $\phi_{\rm m}$ and $\phi_{\rm h}$, may also be attributed to the fact that turbulent scaling laws assume stationarity situations but the SBL is frequently non-stationary due to intermittent turbulence (Klipp and Mahrt, 2004). Zilitinkevich (2002) gives several features that may contribute to the scatter in the data, such as anisotropy of turbulent eddies under stable conditions and the possible effect of baroclinicity. Zilitinkevich and Esau there is little evidence(2003) show from LES data the influence of baroclinicity on turbulent fluxes in the SBL.

Figure 7 shows the behaviour of $\phi_{\rm h}$ for ζ intervals at the heights of 5.8 m, 13.5 m and 32 m. Due to the high standard deviation, any comment about the relationship between $\phi_{\rm h}$ and stability seems less reliable than for $\phi_{\rm m}$. At z=5.8 m there is reasonable agreement for $0.2\leq\ \zeta\ \leq 2$ but below that range $\phi_{\rm h}$ is substantially larger than Businger and other authors findings, although the statistics may not be reliable as some intervals contain only a few points. As for $\phi_{\rm m}$, $\phi_{\rm h}$ levels off for higher stability parameters, $\zeta>2$. At the higher levels, z=13.5 m and 32 m, there is little evidence of the similarity function following Businger's or Webb's functions. In fact, if a detailed analysis of the structure of the ABL is performed when high $\phi_{\rm h}$ values are present with low ζ, a complex structure of the lower atmosphere can be seen which is influenced by the presence of internal waves (Nai-Ping et al., 1983; Rees et al., 2000). These low values of ζ (for the S-period) are not truly neutral points and should not be used to do a fit in this range. If measurements from all nights, not just the S-period, are also included in the analysis, a much better agreement with Businger and Webb is found for low values of ζ (Fig. 8). With regards to the levelling off of $\phi_{\rm h}$ for greater stability ($\zeta>1$–2 approx.) the behaviour is similar to that of $\phi_{\rm m}$, irrespective whether only the S-period is considered or the entire period.

4.3 Relationship between the Richardson number and the stability parameter

The gradient Richardson number, R_i, which was defined in Eq. (8) is a widely used stability parameter relating thermal stratification to wind shear. Nieuwstadt (1984a) considered the relationship between the gradient Richardson number and the stability parameter, ζ, as another example of local-scaling, leading to a functional form $R_i = R_i$ (z/Λ) which is found with the definition of ϕ_m and ϕ_h (Eq. 9). Fig. 9 shows the behaviour of R_i for z=5.8 m, evaluated from Eq. (9) for each point of SABLES98 versus the stability parameter (in Fig. 9a) and then also averaged over the intervals of ζ(Fig. 9b). The results of the present study are consistent with the data shown by Nieuwstadt (1984a). The lines drawn for comparison correspond to Eq. (9) using Businger and Webb functions for ϕ_m and ϕ_h. These functions have a horizontal asymptote for $R_i \approx 0.2$, which is a valid limit for turbulent transfer and which is derived from the values of the similarity functions found by Businger et al. (1971), Högström (1996), and Webb (1970). Other studies (Kondo et al., 1978; Ueda et al., 1981) found a critical value for the flux Richardson number, R_f, of 0.143 and 0.1 respectively. This R_f is related to the ratio of the eddy diffusivities and the gradient Richardson number, $R_f = R_i\ K_h/K_m$. As will be discussed further below, K_h/K_m tends to decrease below 1 for high stability and then the critical R_f is less than the critical R_i, but if the stable boundary layer has continuous turbulence (Nieuwstadt data), then both critical numbers are approximately the same. In spite of our scattered results, the functions found by other studies (Webb, 1970; Businger et al., 1971; Högström, 1996) are inside the error bars calculated from SABLES98. As with the similarity functions, the dimensionless parameter R_i, tends to a constant value in the limit of high values of z/Λ, which is again consistent with z-less stratification.

4.4 Relationship between similarity functions and gradient Richardson number.

As it was commented above, when relationships between turbulent and stability parameters are studied, one problem is self-correlation, i.e. the parameters share one or more variables. This feature was extensively explored by Klipp and Mahrt (2004) who concluded that the gradient Richardson number, R_i, shows less self-correlation with the similarity functions, ϕ_m and ϕ_h, than the stability parameterz Λ. Figure 10 and Fig. 11 show the dependence of ϕ_m and ϕ_h, respectively, on R_i for the three levels analysed (5.8 m, 13.5 m and 32 m) for the whole period, not just the S-period, in order to have more points in a wide range of stability, considering that when R_i is used instead of z/Λ the self-correlation is less.

For weaker stability, $R_i < 0.1$, ϕ_m does not vary significantly with stability while ϕ_h has a positive trend. The ratio

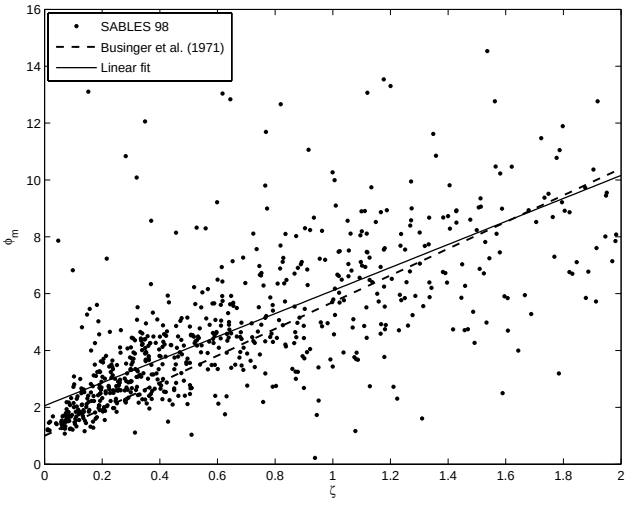

Fig. 6. SABLES98 data and Linear fit of ϕ_m versus ζ for stability parameter <2 at 5.8 m. Businger et al. (1971) function is shown for comparison.

of the mean values in this stability range is $\phi_m/\phi_h > 1$, which decreases to approximately 1 as R_i tends to 0.1. It can be easily deduced (Arya, 2001) that the ratio of the similarity functions, ϕ_m/ϕ_h, is equal to the ratio of the eddy diffusivities for heat and momentum, K_h/K_m. If ϕ_m/ϕ_h decreases with stability, this would imply that the turbulent transfer of heat can be greater than that of momentum for near neutral stabilities.

The evolution for greater stabilities, $R_i > 0.1$, shows that ϕ_m tends to increase with stability and then levels off, or even decreases for the greatest Richardson numbers, while ϕ_h increases to higher values than ϕ_m and then levels off. This evolution produces a $\phi_m/\phi_h < 1$, which would be equivalent to a greater turbulent transfer of momentum compared to the transfer of heat. This result, which is not shown when z/Λ is used as stability parameter, is compatible with the results shown for winter Antarctic data in Yagüe et al. (2001), and has been related in previous works to the presence of internal gravity waves in the atmospheric boundary layer, and associated intermittent processes, using K_m and K_h (Kondo et al., 1978; Wittich and Roth, 1984; Yagüe and Cano, 1994b). These waves can transfer momentum but much less heat, unless they break.

5 Intermittency and mixing in the ABL

Intermittency may be regarded as sharp spikes on the velocity values which affect strongly the higher order moments of the velocity differences. The relationship between kinetic energy and the Richardson number is not simple because stability is very sensible to small wind changes near the surface. Intermittency is often defined in different ways, both for the velocity and scalar turbulent fields (Gibson, 1991), where it

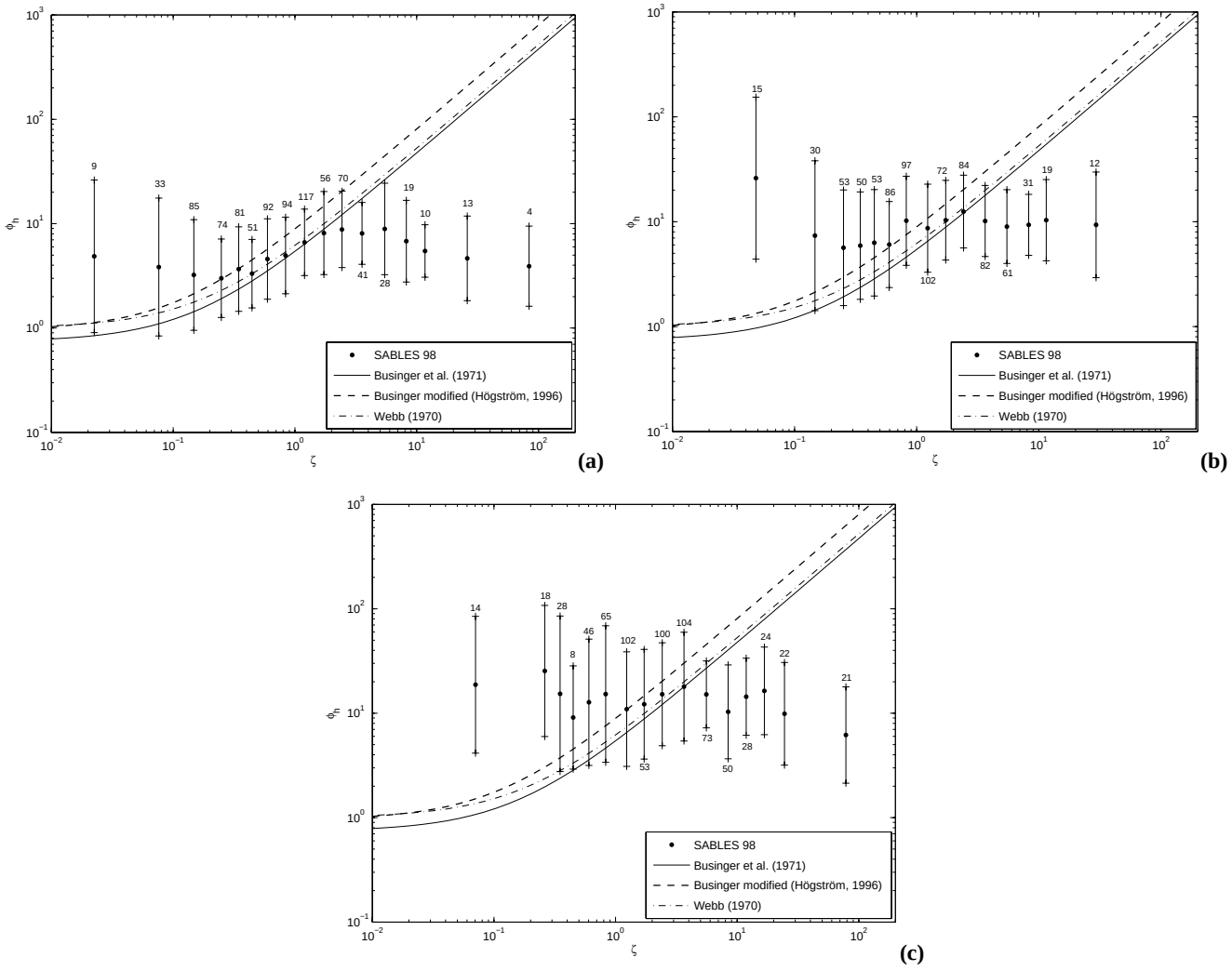

Fig. 7. ϕ_h versus stability parameter grouped into intervals for the S-Period, at: **(a)** 5.8 m, **(b)** 13.5 m and **(c)** 32 m. Functions found by other authors are shown for comparison.

may be considered to produce a "wide tail in a skewed probability density function (PDF)". Kraichnan (1991) discusses further the spectral implications. In general an intermittent turbulent cascade will not exhibit a (-5/3) spectral energy cascade.

A detailed analysis of the turbulence at small scale may reveal intermittent episodes in a stable atmosphere very clearly because of the high Kurtosis of the turbulent velocity PDFs. In this case, under stable stratification conditions, we are able to obtain a better quantification of the intermittency than in a convective situation. A practical way to calculate intermittency as a single parameter can be done following Mahjoub et al. (1998).

The velocity structure function is a basic tool to study the intermittent character of turbulence. The pth order velocity structure function is defined as

$$S_p(l)=\overline{(u(x+l)-u(x))^p} \quad (14)$$

Velocity structure functions require the measurement of velocity at two different locations or times separated a distance l (using Taylor's hypothesis the correspondence between spatial and temporal increments is straightforward with the local mean velocity of the flow at the measured location). In fact, the use of this relation is limited to a low turbulence intensity. More information about the structure functions is given in Frisch (1995) but a small review of some basic ideas and developments in turbulence is at hand to interpret the measurements.

Following Kolmogorov's theory (Kolmogorov, 1941), the self-similarity of the velocity structure function is attained in the inertial range, which is physically defined as a range of scales where both the forcing and the dissipation processes are irrelevant. For the K41 theory (Kolmogorov, 1941), the scaling exponent of the structure functions with separation l is $p/3$. Yet, nonlinearity with a scaling exponent of the

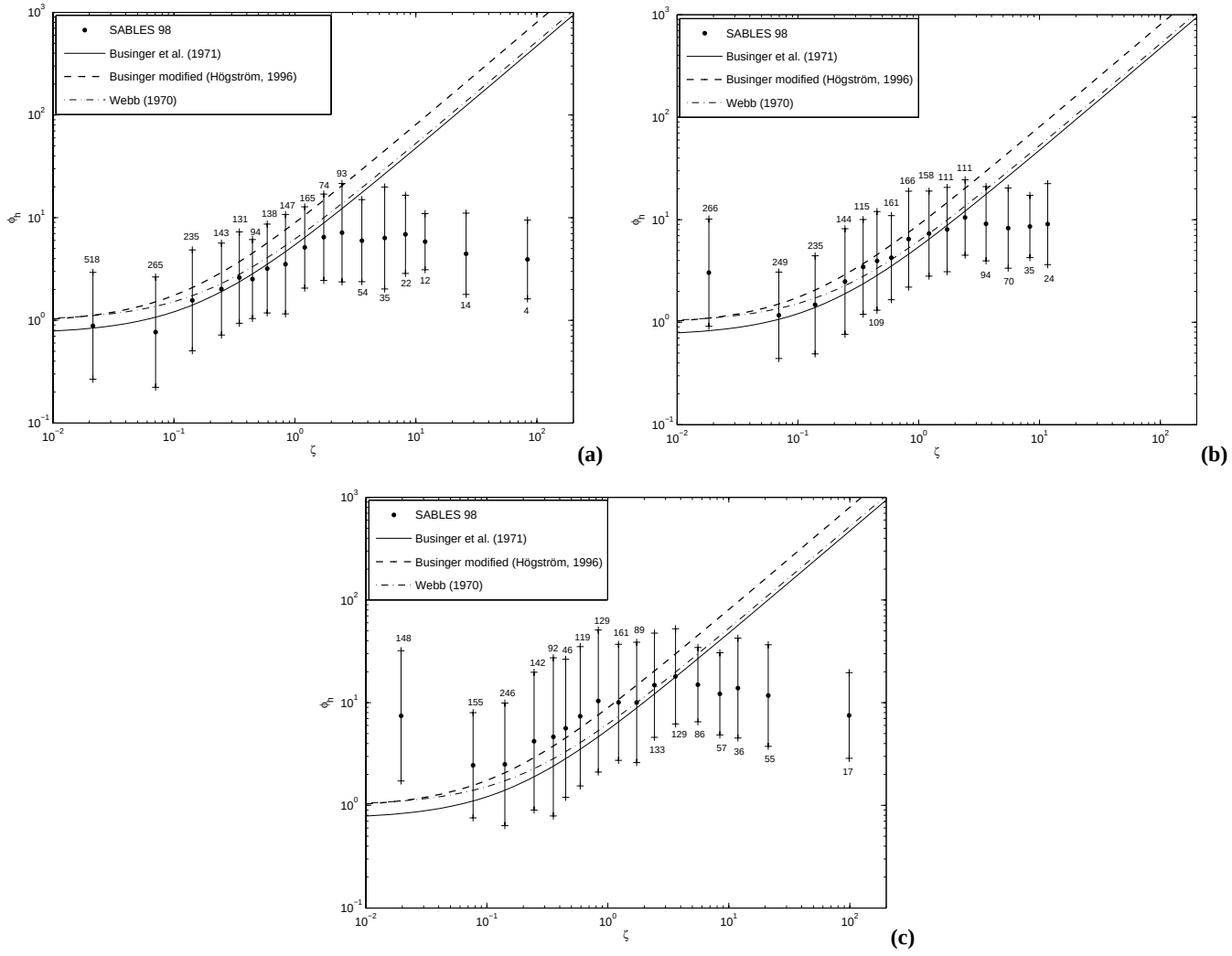

Fig. 8. As Fig. 7, but for the extended nocturnal period from 10 to 26 September.

order p of the statistical moment has been observed in many theoretical, experimental and numerical investigations (see Sreenivasan and Antonia (1997) for a review). In fact, this correction needed in K41 theory is referred to as intermittency, indicating that the average value of the energy dissipation ε will be different at different points in space (Frisch, 1995). The Extended Self Similarity (ESS) property, suggested by Benzi et al. (1993) is a very effective method to determine accurate scaling exponents. Moreover, the existence of ESS could be used as a way to define an inertial range, even in situations where the phenomenological theory suggested by Kolmogorov (1941) and Kolmogorov (1962), known as K62, does not hold. This would apply to situations where there is a strong deviation from local homogeneity and isotropy, such as in the SBL flows (Babiano et al. 1997; Mahjoub et al., 1998). It is important to stress the point that neither K41 nor K62 are valid in non-homogeneous flows such as those in the ABL under strong stratification where non-locality and non-homogeneity effects are indistinguishable from intermittency.

Analysing the turbulence microscale at high sensor resolutions, we can find intermittent episodes in a stable atmosphere. In this case, we are able to obtain a better quantification of the intermittency than in neutral or convective situations. The standard definition of intermittency μ uses the sixth order structure function scaling exponent ξ_6:

$$\mu = 2 - \xi_6 \tag{15}$$

which may be calculated as discussed in Mahjoub et al. (1998) or even in terms of the geometrical structure of the turbulent PDF zero crossings as:

$$\xi_p = \frac{p}{3} + (3 - D)\left(1 - \frac{p}{3}\right) \tag{16}$$

where p is the order of the structure function, in this case p=6, and D is the Fractal dimension. In a similar way, the

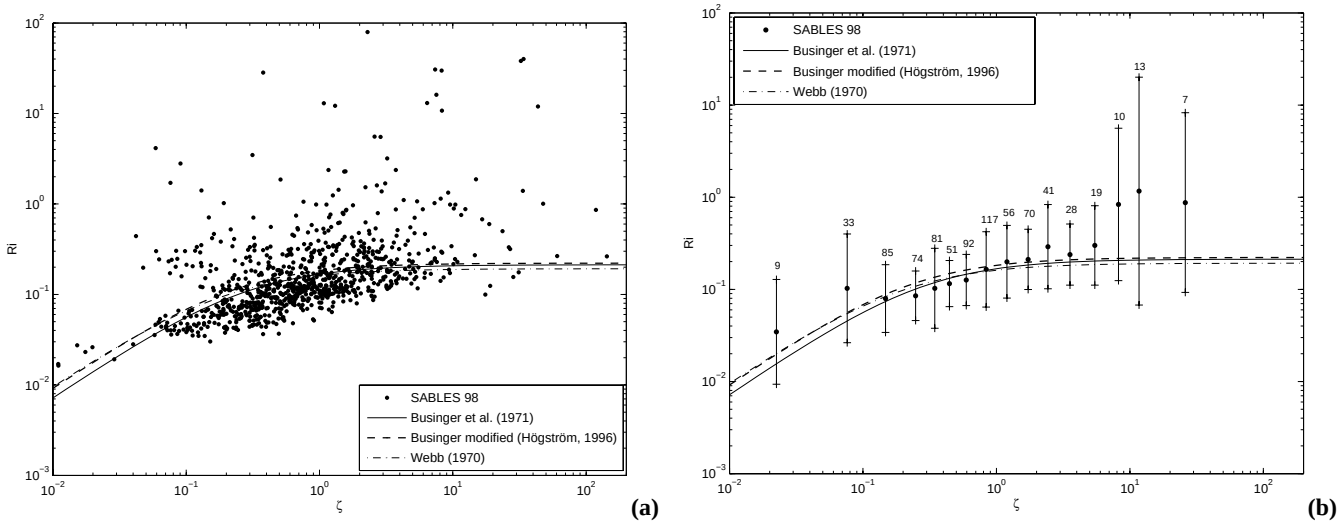

Fig. 9. Richardson number versus ζ for the S-period at z=5.8 m: **(a)** All the individual SABLES98 data, **(b)** interval representation. Functions found by other authors are shown for comparison. Error bars indicate the standard deviation of the individual results contributing to the mean value in each stability bin. The number of samples in each stability bin is given over the upper bar or below it.

fourth order structure function, related to the Kurtosis or flatness, may also be used as a measure of intermittency. Figure 12 compares the cumulative PDF's of a strongly stratified situation in SABLES98 with a neutral one (error function shape) normalized with their respective r.m.s turbulent fluctuations. Two 5 Hz wind speed series from an anemometer placed at z=20 m have been used. The deviations from the Gaussian cumulative PDF are also a direct measure of intermittency; clearly there is much more intermittency for the higher Richardson number situation (strongly stratified). There seems to exist a complex, non-linear relationship between the intermittency, the fractal dimension and the mixing efficiency as discussed by Derbyshire and Redondo (1990).

Both the intermittency and the non-homogeneity produce changes in the spectral energy cascades, related to the second order structure functions, and these will produce strong variations in the mixing efficiency. As a local indicator of the potential energy to kinetic energy ratio, we use the flux and gradient Richardson numbers, R_f and R_i, parameters able to distinguish between different stratification types that also lead to different intermittencies. From the equation of the local turbulent kinetic energy (TKE), comparing buoyancy with the shear production term (the two first terms on the right-hand side):

$$\frac{\partial TKE}{\partial t}=-(\overline{u'w'}\frac{\partial \overline{u}}{\partial z}+\overline{v'w'}\frac{\partial \overline{v}}{\partial z})+\frac{g}{\theta_0}\overline{\theta' w'}-\frac{1}{2}\frac{\partial \overline{u_\alpha'^2 w'}}{\partial z}-\frac{1}{\rho_0}\overline{u'_\alpha \frac{\partial p'}{\partial x_\alpha}}-\varepsilon \quad (17)$$

we obtain the Mixing efficiency or Flux Richardson number (in a reference frame with $\overline{v}$=0):

$$R_f=\frac{g}{\theta_0}\frac{\overline{w'\theta'}}{\overline{u'w'}\frac{\partial \overline{u}}{\partial z}} \quad (18)$$

Considering the following relationships between local fluxes and local gradients introduced first by Boussinesq (1877):

$$\overline{w'\theta'}=-K_h\frac{\partial \overline{\theta}}{\partial z} \quad (19)$$
$$\overline{u'w'}=-K_m\frac{\partial \overline{u}}{\partial z}$$

we obtain that:

$$R_f=\frac{K_h}{K_m}R_i \quad (20)$$

with the gradient Richardson number as defined in (8).

Considering also the Ozmidov scale and the integral length scale of the turbulence we can relate the Richardson numbers in a stratified fluid and their non-linear relationships to the measured universal functions.

The importance of measuring intermittency in internal wave breaking flow is that the use of structure functions and their difference may be used as a test for changes in the spectrum of turbulence from 2-D to 3-D or from a local to a non-local situation. Experiments on irregular waves exhibit much more intermittency than in turbulence produced by regular ones (Mahjoub et al., 1998).

In the two basic formulations K41 and K62, which are strictly speaking only valid for homogeneous and isotropic turbulence, the structure function of the third order related to skewness only takes into account intermittency. The intermittency, defined as a complex structure of the dissipation random field, is reflected in the strongest but rarest events. However, it includes not only a possible contribution of the strongest but rarest fluctuations, but it also extends to the more real situations when the variance of the dissipation

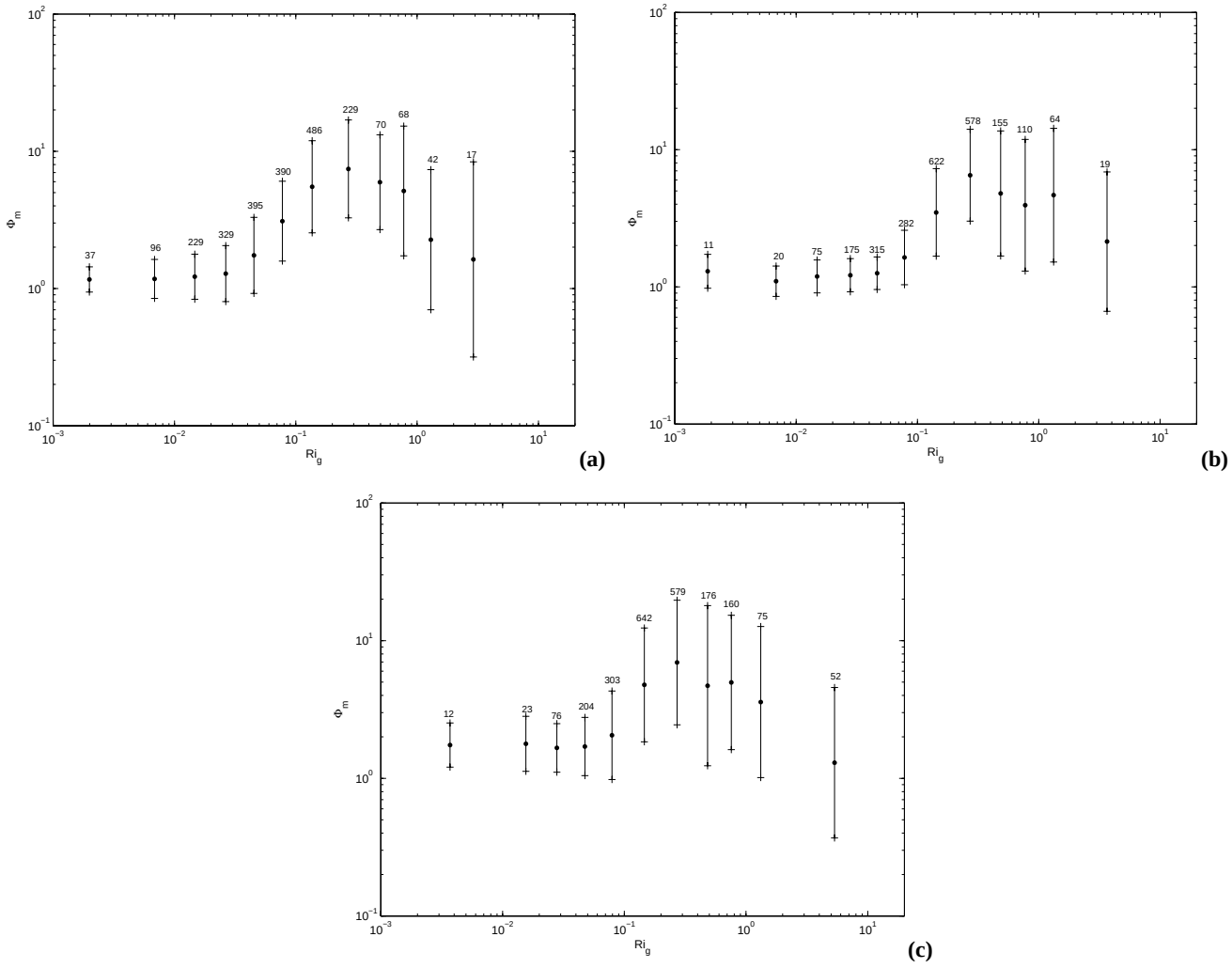

Fig. 10. ϕ_{m} versus gradient Richardson number for the extended nocturnal period from 10 to 26 September grouping in intervals for all stability range at: **(a)** 5.8 m, **(b)** 13.5 m and **(c)** 32 m. Error bars indicate the standard deviation of the individual results contributing to the mean value in each stability bin. The number of samples in each stability bin is given over the upper bar.

changes as a function of the integral length scale of the turbulence as a result of both non-homogeneity in space and anisotropy in different directions producing an anomalous distribution of also the most frequent and smallest fluctuations, and not only of the energetic but rare events, as is the case with the traditional intermittency. In non-homogeneous transfer dynamics, this balance includes both energy transfers from both, larger to smaller scales (normal cascade), and the anomalous energy transfers from smaller to larger scales (inverse cascade). In addition, the true scale-by-scale energy flux is also related to both, the transverse velocity structure and the work of pressure field.

There will be a mixing regime that is different depending on the local stability as it was commented above. The strong turbulent activity can be enough to penetrate the inversion layer and practically destroy it. In the limit of strong turbulence, the Reynolds analogy would apply and the turbulent Prandtl number would tend to unity. But, in other cases the momentum and temperature (or mass) vertical transport may be very different (Carrillo et al., 2001).

It is clear that the transfer of heat and momentum, as well as the TKE, are well controlled by the gradient Richardson number. For very stable ranges, the coefficients are almost of the order of 1/1000. It is also interesting that $K_h/K_m<1$ for strong stability. This is an indication of internal-gravity waves activity which can produce transfer of momentum but little transfer of heat if these waves do not break. The local turbulent parameters are also highly dependent on the friction velocity and on the inversion strength.

The behaviour of turbulence in the Atmospheric Boundary layer is strongly affected by stability; it is possible to relate the Richardson number to the geometrical aspect of a density interface using fractal geometry and apply the relationship between intermittency and fractal structure to the

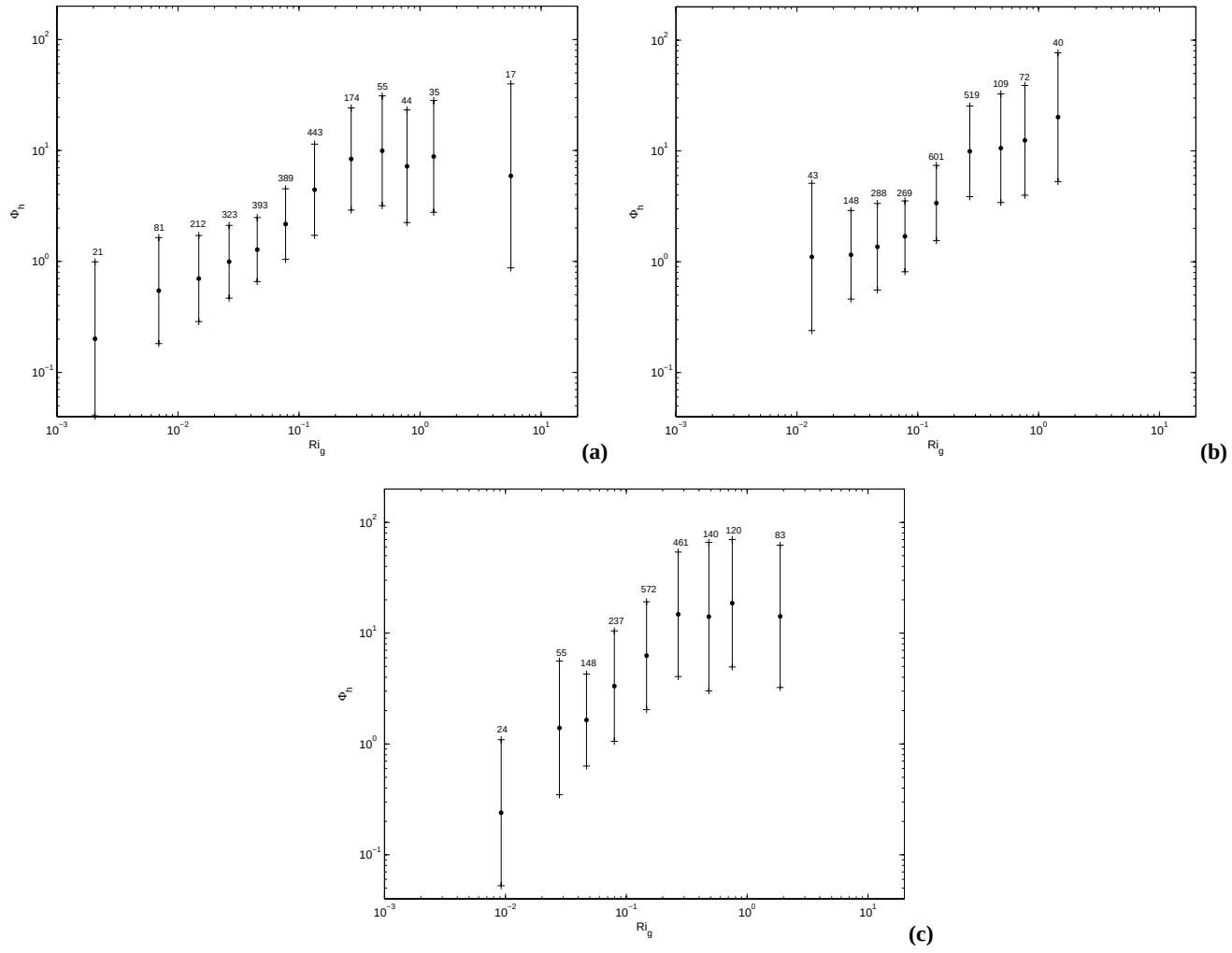

Fig. 11. As Figure 10, but for ϕ_{h}.

atmospheric data. The functional relationships are not conclusive due to the difficulty in the calculation of higher order moments but intermittency clearly increases with higher stability. The effect of stratification on the inverse turbulent Prandtl number, which is a dimensionless number defined as the ratio of the eddy diffusivity for heat to momentum K_h/K_m has been studied in many laboratory experiments, and this number decreases as stability (Richardson number) increases for strong stratifications, showing the difference between the turbulent mixing of momentum and heat. Sometimes this difference is ignored for simplicity but this leads to an underestimation of turbulent momentum transport at stable conditions. The observed behaviour supports the idea that under strong stable conditions (marked by high Richardson number, even greater than the critical 0.25) mixing of heat is inhibited to a greater extent compared to that of momentum. The role of internal gravity waves in this situation of intermittent and sporadic turbulence seems responsible for the more efficient transfer of momentum.

6 Summary and conclusions

The influence of local stability, as measured by the stability parameter ζ=z/Λ and the gradient Richardson number, on the non-dimensional gradients of wind speed and temperature, ϕ_{m} and ϕ_{h}, respectively, has been studied using data from the experiment SABLES98 for a wide range of stability (from weak to strong). When no direct measurements (from sonic anemometers) are available, the universal similarity functions ϕ_{m} and ϕ_{h} for non-dimensional wind and temperature profiles must be known in order to estimate the surface fluxes. The importance of the behaviour of these functions is in relation to describe these surface fluxes which are key parameters in the atmospheric circulation models and dispersion models. For weak to moderate stability the linear functions, widely used in the literature, are valid but for strong stability high errors can be produced if the surface fluxes are estimated from these linear functions. The different behaviour of the momentum and heat turbulent mixing

for strong stability has been analysed, and the influence of intermittency on this very stable regime has been discussed. A number of conclusions can be drawn from the present work:

1. The general behaviour (though with greater scatter for ϕ_h) obtained in the relationships between the similarity functions, ϕ_m and ϕ_h, and z/Λ is an increase with stability up to a certain value ($\zeta > 1$–2approx.),above which ϕ_m and ϕ_h tend to level off, staying almost constant for greater stabilities. For these higher stabilities, the differences between SABLES98 data and Businger et al. (1971) functions become substantial. The best agreement is found at the lowest level (z=5.8 m) which could be related to the reduced intermittency closer to the ground.

2. A linear fit of ϕ_m versus z/Λ to SABLES98 data for the three heights considered (5.8 m, 13.5 m and 32 m) and for $\zeta < 2$, showed a decreasing slope with height. This result supports the importance of using local-scaling even when stability is weak to moderate.

3. For weak stability, $\zeta < 0.1$, ϕ_h showed unexpectedly large values for the S-period, especially at the higher levels which could be related to the interaction of turbulence with internal waves. This interaction results in rapid local mixing and would give low values of ζ even in an overall context of stable stratification, as it is the case for this S-period. When many near-neutral data are introduced in the analysis, this phenomenon is masked by averaging with lower values for ϕ_h obtained from the lower stability periods.

4. The use of the common linear similarity functions for $\zeta > 1$ can produce overestimation of the ϕ_m and ϕ_h values and a corresponding underestimation of the surface fluxes. Such an error in their estimates would affect the reliability of atmospheric circulation models and dispersion models where this information is used to evaluate the turbulent fluxes and other parameters.

5. The relationships between ϕ_m, ϕ_h and the gradient Richardson number have also been studied. Some authors (Klipp and Mahrt, 2004) have pointed out that self-correlation between the similarity functions and the gradient Richardson number, R_i, would be much less of an issue than between the similarity functions and the stability parameter, ζ. SABLES98 results revealed differences in the behaviour of ϕ_m versus R_i compared to that of ϕ_h, which provides insight in the relative magnitude of momentum transfer to heat transfer. For high stabilities it was found that ϕ_m/ϕ_h is less than 1, which would be equivalent to a greater transfer of momentum compared to the transfer of heat, which can also be related to the nonlinear Prandtl number. This change in the ratio could be related to the presence of internal-gravity waves and resulting intermittency in the SBL.

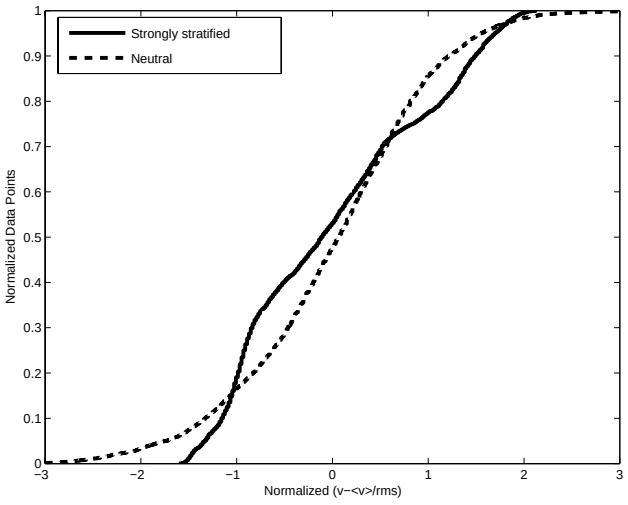

Fig. 12. Comparison of the cumulative normalized PDF of a neutral situation (dashed line) with low Richardson number and of a strongly stratified situation (solid line). The deviations from the error function at 2–4 r.m.s. values indicate the intermittency produced by internal wave bursts.

For an estimate of the intermittency, the cumulative PDF of a strongly stratified situation was compared to a neutral case. The deviations from the Gaussian cumulative PDF are a direct measurement of intermittency which is found for large values of Richardson number.

Acknowledgements. This research has been funded by the Spanish Ministry of Education and Science (projects CLI97-0343 and CGL2004-03109/CLI). We are also indebted to all the team participating in SABLES98 and Prof. Casanova, Director of the CIBA, for his kind help. Thanks are also due to Dr. Früh for his constructive remarks. Comments from Dr. Esau and the two anonymous referees are also appreciated.

Edited by: W. G. Früh
Reviewed by: three referees

References

Arya, S. P. S.: Introduction to Micrometeorology, 2nd edition, International Geophysics Series, Academic Press, London., 2001.

Babiano, A., Dubrulle, B., and Frick, P.: Some properties of two dimensional inverse energy cascade dynamics, Phys. Rev. E., 55, 2693–2706, 1997.

Basu, S.: Large-eddy simulation of the stably stratified atmospheric boundary layer turbulence: a scale-dependent dynamic modelling approach, PhD Thesis, Department of Civil Engineering, University of Minnesota, 114, 2004.

Beljaars, A. C. M. and Holtslag, A. A.: Flux parameterization over land surfaces for atmospheric models, J. Appl. Meteorol., 30, 327–341, 1991.

Benzi R., Ciliberto S., Tripiccione R., Baudet, C., Masssaioli, F., and Succi, S.: Extended self-similarity in turbulent flows, Phys. Rev. E., 48, 29–32, 1993.

Berman, S., Ku, J. Y., Zhang, J., and Trivikrama, R.: Uncertainties in estimating the mixing depth. Comparing three mixing depth models with profiler measurements, Atmos. Environ., 31, 3023–3039, 1997.

Boussinesq, J.: Essai sur la theorie des eaux courants, Mem. Pres. Par div. Savants a l'Academie Sci., Paris, 23, 1–680. 1877.

Businger, J. A., Wyngaard, J. C., Izumi, Y., and Bradley, E. F.: Flux-profile relationships in the atmospheric surface layer, J. Atmos. Sci., 28, 181–189, 1971.

Carrillo, A., Sanchez, M. A., Platonov, A., and Redondo, J. M: Coastal and Interfacial Mixing. Laboratory Experiments and Satellite Observations, Physics and Chemistry of the Earth, part B, 26, 305–311, 2001.

Cheng, Y. and Brutsaert, W.: Flux-profile relationships for wind speed and temperature in the stable atmospheric boundary layer, Bound-Layer Meteorol., 114, 519–538, 2005.

Cuxart, J., Yagüe, C., Morales, G., Terradellas. E., Orbe, J., Calvo, J., Fernandez, A., Soler, M. R., Infante, C, Buenestado, P., Espinalt, A., Joergensen, H. E., Rees, J. M., Vilà, J., Redondo, J. M., Cantalapiedra, I. R., and Conangla, L.: Stable Atmospheric Boundary Layer Experiment in Spain (SABLES 98): A report, Bound-Layer Meteorol., 96, 337–370, 2000.

Cheng, Y. and Brutsaert, W.: Flux-profile relationships for wind speed and temperature in the stable atmospheric boundary layer, Bound-Layer Meteorol., 114, 519–538, 2005.

Derbyshire, S. H.: Stable boundary-layer modelling: Established approaches and beyond, Bound-Layer Meteorol., 90, 423–446, 1999.

Derbyshire, S. H. and Redondo, J. M.: Fractals and waves, some geometrical approaches to stably-stratified turbulence, Anales de Física, Serie A, 86, 67–76, 1990.

Duynkerke, P. G.: Turbulence, radiation and fog in Dutch stable boundary layers, Bound-Layer Meteorol., 90, 447–477, 1999.

Dyer, A. J.: A review of flux-profile relationships, Bound-Layer Meteorol., 7, 363–372, 1974.

Esau, I. N.: Parameterization of a surface drag coefficient in conventionally neutral planetary boundary layer, Ann. Geophys. 22, 3353–3362, 2004.

Finnigan, J. J., Einaudi, F., and Fua, D.: The interaction between an internal gravity wave and turbulence in the stably-stratified nocturnal boundary layer, J. Atmos. Sci., 41, 2409–2436, 1984.

Forrer, J. and Rotach, M. W.: On the turbulence structure in the stable boundary layer over the Greenland Ice Sheet, Bound-Layer Meteorol., 85, 111–136, 1997.

Frisch, U.: Turbulence: The legacy of A. N. Kolmogorov, Cambridge University Press, 1995.

Gibson, C. H.: Kolmogorov similarity hypotheses for scalar fields: sampling intermittent turbulent mixing in the ocean and galaxy, Proc. R. Soc. Lond. A 434, 149–164, 1991.

Grachev, A. A., Fairall, C. W., Persson, P. O. G., Andreas, E. L., and Guest, P. S.: Stable boundary-layer scaling regimes: The Sheba Data., Bound-Layer Meteorol., 116, 201–235, 2005.

Handorf, D., Foken, T., and Kottmeier, C.: The stable atmospheric boundary layer over an antarctic ice sheet, Bound-Layer Meteorol., 91, 165–189, 1999.

Hicks, B. B.: Wind profile relationships from the Wangara experiments, Quart. J. Roy. Meteorol. Soc., 102, 535–551, 1976.

Högström, U.: Non-dimensional wind and temperature profiles in the atmospheric surface layer: A re-evaluation, Bound-Layer Meteorol., 42, 55–78, 1988.

Högström, U.: Review of some basic characteristics of the atmospheric surface layer, Bound-Layer Meteorol., 78, 215–246, 1996.

Howell, J. F. and Sun, J.: Surface-layer fluxes in stable conditions, Bound.-Layer Meteorol., 90, 495–520, 1999.

Jacobson, M. Z.: Atmospheric Pollution: History, Science and Regulation, Cambridge University Press, Cambridge, 2002.

King, J. C.: Some measurements of turbulence over an antarctic shelf, Quart. J. Roy. Meteorol. Soc., 116, 379–400, 1990.

King, J. C. and Anderson, P. S.: Installation and performance of the STABLE instrumentation at Halley, British Antarctic Survey Bulletin, 79, 65–77, 1988.

King, J. C. and Anderson, P. S.: Heat and water vapour fluxes and scalar roughness lengths over an antarctic ice shelf, Bound.-Layer Meteorol., 69, 101–121, 1994.

Klipp, C. L. and Mahrt, L: Flux-gradient relationship, self-correlation and intermittency in the stable boundary layer, Quart. J. Roy. Meteorol. Soc., 130, 2087–2103, 2004.

Kolmogorov, A. N.: Local structure of turbulence in an incompressible fluid at very high Reynolds numbers, Dokl. Accad Nauk. URSS, 30,299–303, 1941.

Kolmogorov, A. N: A refinement of previous hypotheses concerning the local structure of turbulence in a viscous incompressible fluid at high Reynolds number, J. Fluid Mech., 13, 82–85, 1962.

Kondo, J., Kanechica, O., and Yasuda, N.: Heat and momentum transfers under strong stability in the atmospheric surface layer, J. Atmos. Sci., 35, 1012–1021. 1978.

Kraichnan, R. H.: Turbulent cascade and intermittency growth, Proc. R. Soc. Lond. A, 434, 65–78, 1991.

Lange, B., Larsen, S., Hojstrup, J., and Barthelmie, R.: The influence of thermal effects on the wind speed profile of the coastal marine boundary layer, Bound.-Layer Meteorol., 112, 587–617, 2004.

Launiainen, J.: Derivation of the relationships between the Obukhov stability parameters and bulk Richardson number for flux-profiles studies, Bound.-Layer Meteorol.,76, 165–179, 1995.

Lee, H. N.: Improvement of surface flux calculations in the atmospheric surface layer, J. Appl. Meteorol., 36, 1416–1423, 1997.

Louis, J. F.: A parametric model of vertical eddy fluxes in the atmosphere, Bound.-Layer Meteorol., 17, 187–202, 1979.

Mahjoub, O. B., Babiano A. and Redondo, J. M.: Structure functions in complex flows, Flow, Turbulence and Combustion, 59, 299–313, 1998.

Mahrt, L.: Intermittency of atmospheric turbulence, J. Atmos. Sci, 46, 79–95, 1989.

Mahrt, L.: Stratified atmospheric boundary-layers, Bound.-Layer Meteorol., 90, 375–396, 1999.

Mahrt, L., Sun, J, Blumen, W., Delany, A., McClean, G., and Oncley, S.: Nocturnal boundary-layer regimes, Bound-Layer Meteorol., 88, 255–278, 1998.

Monin, A. S. and Obukhov, A. M.: Basic laws of turbulent mixing in the ground layer of the atmosphere, Akad. Nauk SSSR, 151, 163–187, 1954.

Morgan, T. and Bornstein, R. D.: Inversion climatology at San Jose, California, Mon. Weather Rev., 105, 653–656, 1977.

Nai-Ping, L., Neff, W. D., and Kaimal, J. C.: Wave and turbulence structure in a disturbed nocturnal inversion, Bound-Layer Meteorol., 26, 141–155, 1983.

Nieuwstadt, F. T. M.: Some aspects of the turbulent stable boundary layer, Bound-Layer Meteorol., 30, 31–55, 1984a.

Nieuwstadt, F. T. M.: The turbulent structure of the stable nocturnal boundary layer, J. Atmos. Sci., 41, 2202–2216, 1984b.

Noguer, M., Jones, R., and Murphy, J.: Sources of systematic errors in the climatology of a regional climatic model over Europe, Clim. Dynam., 14, 691–712, 1998.

Obukhov, A. M.: Turbulence in an atmosphere with inhomogeneous temperature, Tr. Inst. Teor. Geofis. Akad. Nauk. SSSR, 1, 95–115, 1946, English translation in Bound.-Layer Meteorol., 2, 7–29, 1971.

Poulos, G. S., Blumen, W., Fritts, D. C., Lundquist, J. K., Sun, J., Burns, S. P., Nappo, C., Banta, R., Newsom, R. Cuxart, J., Terradellas, E., Balsley, B., and Jensen, M.: CASES-99: A comprehensive investigation of the stable nocturnal boundary layer, Bull. Amer. Meteorol. Soc., 83, 555–581, 2002.

Redondo, J. M., Sánchez, M. A., and Cantalapiedra, I. R.: Turbulent mechanisms in stratified fluids, Dyn. Atmos. Oceans, 24, 107–115, 1996.

Rees, J. M., Denholm-Price, J. C. W., King, J. C., and Anderson, P. S.: A climatological study of internal-gravity waves in the atmospheric boundary layer, J. Atmos. Sci., 57, 511–526, 2000.

Rodríguez, A., Sánchez-Arcilla, A., Redondo, J. M., Bahia, E., and Sierra, J. P.: Pollutant dispersion in the nearshore region: modelling and measurements, Water Science and Technology, 32, 169–178, 1995.

Sharan, M., Rama Krishna, T. V. B. P. S., and Aditi: On the bulk Richardson number and flux–profile relations in an atmospheric surface layer under weak wind stable conditions, Atmos. Environ., 37, 3681–3691, 2003.

Sodemann, H. and Foken, T.: Empirical evaluation of an extended similarity theory for the stably stratified atmospheric surface layer, Quart. J. Roy. Meteorol. Soc., 130, 2665–2671, 2004.

Sreenivasan, K. R. and Antonia, R. A.: The phenomenology of small-scale turbulence, Ann. Rev. Fluid Mech., 29, 435–472, 1997.

Sugita, M. and Brutsaert, W.: The stability functions in the bulk similarity formulation for the unstable boundary layer, Bound-Layer Meteorol., 61, 65–80, 1992.

Ueda, H., Mitsumoto, S., and Komori, S.: Buoyancy effects on the turbulent transport processes in the lower atmosphere, Quart. J. Roy. Meteorol. Soc., 107, 561–578, 1981.

Webb, E. K.: Profile relationships: The log-linear range and extension to strong stability, Quart. J. Roy. Meteorol. Soc., 96, 67–90,1970.

Wittich, K. P. and Roth, R.: A case study of nocturnal wind and temperature profiles over the inhomogeneous terrain of Northern Germany with some considerations of turbulent fluxes, Bound-Layer Meteorol., 28, 169–186, 1984.

Wyngaard, J. C.: On surface layer turbulence, in: Workshop in Micrometeorology, edited by: Haugen, D. A., Am. Meteorol. Soc., 105–120, 1973.

Yagüe, C. and Cano, J. L.: Eddy transfer processes in the atmospheric boundary layer, Atmos. Environ., 28, 1275–1289, 1994a.

Yagüe, C. and Cano, J. L.: The influence of stratification on heat and momentum turbulent transfer in Antarctica, Bound-Layer Meteorol., 69, 123–136, 1994b.

Yagüe, C. and Redondo, J. M.: A case study of turbulent parameters during the Antarctic winter, Antarc. Sci., 7, 421–433, 1995.

Yagüe, C., Maqueda, G., and Rees, J. M.: Characteristics of turbulence in the lower atmosphere at Halley IV station, Antarctica, Dyn. Atmos. Oceans, 34, 205–223, 2001.

Yagüe, C., Morales, G., Terradellas, E., and Cuxart, J.: Turbulent mixing in the stable atmospheric boundary layer, Ercoftac Bulletin, 60, 53–57, 2004.

Zilitinkevich, S. S.: Third-order transport due to internal gravity waves and non-local turbulence in the stably stratified surface layer, Quart. J. Roy. Meteorol. Soc., 128, 913–925, 2002.

Zilitinkevich, S. S. and Chailikov , D. V.: Determining the universal wind velocity and temperature profiles in the atmospheric boundary layer, Izvestiya, Atmos. Ocean. Phys., 4, 165–170, 1968.

Zilitinkevich, S. S. and Calanca, P.: An extended similarity theory for the stably stratified atmospheric surface layer, Quart. J. Roy. Meteorol. Soc., 126, 1913–1923, 2000.

Zilitinkevich, S. S. and Esau, I. N.: The effect of baroclinicity on the equilibrium depth of the neutral and stable planetary boundary layers, Quart. J. Roy. Meteorol. Soc., 129, 3339–3356, 2003.